Updating Chinese SO_2 emissions with surface observations for regional air-quality modeling over East Asia

Changhan Bae[1]†, Hyun Cheol Kim[2,3,]†, Byeong-Uk Kim[4], Younha Kim[5], Jung-Hun Woo[5] and Soontae Kim[1]

[1]Department of Environmental and Safety Engineering, Ajou University, Suwon, South Korea

[2]Air Resources Laboratory, National Oceanic and Atmospheric Administration, College Park, MD, USA

[3]Cooperative Institute for Satellite Earth System Studies, University of Maryland, College Park, MD, USA

[4]Georgia Environmental Protection Division, Atlanta, GA, USA

[5] Dept. of Advanced Technology Fusion, Konkuk University, Seoul, South Korea

† Both authors contributed equally

Correspondence to: Soontae Kim (soontaekim@ajou.ac.kr), Hyun Cheol Kim (hyun.kim@noaa.gov)

Abstract. Anthropogenic emissions in East Asia have changed dramatically in recent years. To measure these changing emissions in support of air-quality modeling, we developed a top-down emission update system using surface observations and a geographical information system spatial-allocation technique. We deploy a data-processing system to construct adjustment factors to prefecture-level SO_2 emissions by comparing surface and modeled observations. A case study is conducted over East Asia for 2016 in which we update Chinese SO_2 emissions using measurements from around 1500 surface monitoring sites. Model simulations using updated SO_2 emissions are improved relative to the existing simulation system (e.g., R=0.23 to R=0.8), suggesting that the newly designed system provides an efficient, practical forecast solution. Finally, estimated SO_2 emissions are compared with existing emission inventories, agreeing well with recent reports of reduced SO_2 emissions from Chinese anthropogenic sources.

1. Introduction

In any region with rapidly developing countries, such as East Asia, the amount of sulfur dioxide (SO_2) released into the atmosphere offers a good indicator for fast-paced changes in industrialization and urbanization (Xiao et al., 2018). Much SO_2 in the atmosphere derives from human sources (Klimont et al., 2013), usually power generation and industrial activities, including combustion of sulfur-containing fuels and the processing of materials containing sulfur (such as oil refining and metal smelting) (Stern, 2005). Volcanic eruptions and degassing are major natural sources (Flower et al., 2016; Krueger et al., 2008).

High SO_2 concentrations are associated with many environmental impacts. SO_2 is an invisible, toxic gas with a sharp smell that directly affects human health (Chen et al., 2012), especially the respiratory system. Tropospheric SO_2 is also a major precursor to fine particulate matter (PM), as it forms sulfate particles (Park and Cho, 1998; Qu et al., 2016; Ying et al., 2014). It impairs visibility (Lin et al., 2012), harms vegetation, decreases plant growth and yield, and contaminates soil as acid rain. Its impact on climate has also been reported (Harris et al., 2013; Lin et al., 2013).

China has experienced increasing air pollution for several decades. Chinese SO_2 emissions have been very high, especially over areas with rapid industrialization and urbanization. In China, power generation and the industrial sectors are major emissions sources (Liu et al., 2016); the residential sector is also important in the northern provinces due to demand for residential heating. However, China has recently reversed the trend in its SO_2 emissions, especially since 2006, as the Chinese government has implemented legislation to mitigate extreme air pollution (Liu et al., 2012; Schreifels et al., 2012; van der A et al., 2017). Stringent emissions control policy, the application of improved combustion technologies, and the promotion of renewable energy technologies have successfully controlled emissions, as recent studies have reported (Silver et al., 2018; van der A et al., 2017; Wang et al., 2018; Zheng et al., 2018). With reduced OMI (Ozone Monitoring Instrument)-measured SO_2 column densities over Beijing and surrounding provinces in 2008, Huanhuan et al. (2014) argued that strict controls on pollutant emissions and motor vehicle traffic before and during the 2008 Olympic and Paralympic Games were effective (Huanhuan et al., 2014). Over China, SO_2 emissions reportedly increased until the middle of 2000. Krotkov et al. (2016) reported a decreasing trend over the North China Plain since 2011, with about a 50% reduction from 2012 to 2015, and suggested that the economic slowdown and government efforts to restrain emissions from the power and industrial sectors explain this change (Krotkov et al., 2016). While accurate information on SO_2 emissions (their location and amount) is required to establish air-quality models for forecasting and policymaking, such information has been difficult to obtain, especially in near real-time. The amount of anthropogenic emissions in China seem to be determined partly by the balance between increasing energy consumption and the efficiency of government emission-control policies and partly by natural fluctuations (Kang et al., 2019; Kim et al., 2017; Miao et al., 2017). Estimating anthropogenic emissions in China is therefore difficult because so many factors contribute to overall emissions (Li et al., 2017a).

In traditional bottom-up approaches, SO_2 emissions inventories are estimated from actual measurements (such as continuous emission monitors at major electricity-generating sites), emission factor estimation for other fuel combustion sources and industrial processes, and model simulations for on-road and non-road sources (EPA, 2008). To establish bottom-up emissions, comprehensive parameters are required for fuel consumption, industrial production, emission factors, and control efficiency (Li et al., 2017b). While the bottom-up approach can provide detailed information on anthropogenic emissions, establishing a complete emissions inventory takes many resources and much time, which limits the ability of such an inventory to meet the demands of real-time modeling systems (Wang et al., 2016).

To estimate the amount of SO_2 emissions, the top-down approach is an alternative that uses observed information to constrain total estimated emissions. Using space-borne measurements to estimate the anthropogenic emissions from the surface has become very popular in the simulation of regional air quality thanks to its advantage in spatial coverage (Fioletov et al., 2016; Koukouli et al., 2018; Liu et al., 2018; Qu et al., 2019). Multiple space-borne instruments can monitor changes in both anthropogenic (Krotkov et al., 2016; Zhang et al., 2017) and natural emissions (Krueger et al., 2008; Spinei et al., 2010; Theys et al., 2019) from regional and global sources, including SO_2 signals from anthropogenic sources. Several studies have shown how emissions have evolved from very large source regions, such as China. However, although space-borne monitoring has the advantage of offering wide coverage, satellite-based approaches have limitations resulting from data-retrieval uncertainty or errors in the conversion of columnar to surface information (Fioletov et al., 2017, 2013; Georgoulias et al., 2009; Koukouli et al., 2016; Lee et al., 2011).

In this study, we examine an alternative approach to updating top-down SO_2 emissions. Recently, more surface-monitoring networks have been developed in China with a very dense distribution of coverage. Taking advantage of these networks, we tested an alternative approach to estimate SO_2 emissions from anthropogenic sources over China. Section 2 describes the data and emission adjustment method. Estimation of emission adjustments and model simulations are discussed in Section 3, and Section 4 concludes.

2. Data & Methodology

2.1. Observations

Surface observation data were obtained from the China National Environmental Monitoring Center (CNEMC; data available at http://www.pm25.in). The website distributes hourly concentrations of PM_{10}, $PM_{2.5}$, CO, NO_2, O_3, SO_2, and Air Quality Indices from more than 1500 surface-monitoring sites across China. As of 2016, observations are available from 1571 sites; 1459 sites are within our study domain. After discarding 127 sites by screening for observation sites with less than 80% of values available, we used observations from 1332 sites in the analysis.

2.2. Model

Meteorological and chemistry-transport models are used to simulate regional air quality over an East Asian domain. Weather Research and Forecasting Model (WRF) version 3.4.1 was used to simulate meteorology (Skamarock and Klemp, 2008), initiated with the National Centers for Environmental Protection (NCEP) Final

Analysis (FNL) product.(NCEP, 2000) Community Multiscale Air Quality (CMAQ) was used to simulate chemistry transport (Byun and Schere, 2006), with meteorological inputs processed through the Meteorology–Chemistry Interface Processor (MCIP) version 3.6 (Otte and Pleim, 2010); emissions were processed using Sparse Matrix Operator Kernel Emission (SMOKE). We used AERO5 aerosol module and Statewide Air Pollution Research Center version 99 (SAPRC99) as the chemical mechanisms in the chemical transport model (Carter, 2003). **Table 1** lists detailed information on modeling configurations. The base model simulation was conducted using the Comprehensive Regional Emissions Inventory for Atmospheric Transport Experiment (CREATE) 2015 (Jang et al., 2019).

2.3. Method

Ratios between observed and modeled surface SO_2 concentrations are calculated as follows. We constructed a spatial distribution of surface SO_2 concentrations using surface and satellite observations. For each month and prefecture, we calculate the adjustment ratio to Chinese emissions sources from surface and model concentrations, as follows:

$$E_{SO2,adj} = E_{SO2,mod} \cdot \frac{C_{SO2,obs}}{C_{SO2,mod}}$$

Emissions on cells with multiple prefectures are calculated using the fractional weight of each adjacent prefecture's emissions using the conservative re-gridding method (Kim et al., 2018; Kim et al., 2016).

We followed the following simple rules:

- We honor basic information from the current emission inventory.
- We discarded hourly observational data sets with more than 20% of values missing. We also did a fair sampling of observations and model simulations by discarding any of paired observations and model has missing values.
- Observations allocated within the same domain (grid) cell were merged together. We averaged such observations because we do not want to over-weight dense monitoring sites, which are usually at urban locations.
- All observations within a prefecture were merged to calculate the average. Using this information, we estimated one adjustment ratio for each prefecture. This practical data-processing approach is justified by the following assumptions: (1) policy implementation tends to be conducted by administrative group; (2) SO_2 observations within a prefecture represent local emissions and the airborne concentrations; (3) provinces are too large to be considered as a single factor; and (4) analysis at the prefecture level reduces the effects from transport; and
- Spatial representativeness can be a problem in data processing. Applying more advanced spatial re-gridding techniques, such as kriging or machine learning, can help.

In total, after merging data from 1332 monitoring sites into domain cells, around 550 observations were used to calculate the adjustment ratios. We assigned surface-monitoring observations to prefecture-level concentration using the Database of Global Administrative Areas (GADM; https://gadm.org/), which provides high-resolution data for country administrative areas.

Compared to the top-down method of estimating emissions based on satellite, space-borne observations, using surface-based observations to make top-down estimates has both benefits and limitations. Since we focus on the construction of accurate emissions input to improve the performance of regional air-quality modeling, surface observational data can provide a more realistic emissions input by focusing on the chemical behaviors of ground-level pollutants. Moreover, and again compared to satellite products, surface observations have much less potential retrieval uncertainty. In estimating ground-level emission sources, ground-level data are less affected by transport compared to satellite data, which uses information about column-integrated density. The surface data we used in this study also offer better temporal coverage compared to a polar-orbiting satellite product with limited local overpass time.

On the other hand, surface observations are clearly limited in their spatial coverage and can be spatially unrepresentative, potentially missing information over areas without monitoring sites or over-emphasizing local pollutants detected by monitors located near local hotspots of SO_2 emissions. This method may notably overfit the deficiencies of the model itself into emission adjustments, since meteorological and chemical models are not perfect; the model can attribute those imperfections into emission adjustments that are, in reality, non-emission factors.

3. Results

3.1. Base simulation

Before we applied the top-down emissions adjustment, we conducted a base case simulation using the CREATE 2015 emissions inventory. **Figure 1** shows the spatial distribution of modeled and observed surface SO_2 concentrations over China during June 2016. As expected, high concentrations were found over Northern China, especially over the Beijing, Tianjin, and Hebei (BTH) region, which forms the core of China's recent rapid industrialization. Strong signals of SO_2 concentrations are shown over Tianjin and southern Hebei, extending to surrounding provinces of the BTH region, such as Shandong, Shanxi, Henan, and Inner Mongolia. Elevated SO_2 concentrations are also shown in areas near the Yangtze Delta River (YDR) region, as well as over Jiangsu, Anhui, and Zhejiang provinces. Over western China, the high SO_2 concentrations around Chongqing municipality represent the region's industrialization. **Figure 1b** shows the spatial distribution of bias (that is, modeled concentrations less observations) for the same period. The bias patterns display several noticeable discrepancies, mostly over the east coast mega cities. We attribute these biases to the failures of the emissions inventory to keep up with recent changes in released emissions, which is very common when using bottom-up emissions inventories. We think the approach presented in this paper can complement these shortcomings of the current emission inventory. Major overestimation of SO_2 emissions in the model occurs in the YRD and the BTH. Emissions from the Pearl River Delta (PRD), another location with large biases in the model, are not recognized in **Figure 1a**.

3.2. Estimation of adjustment ratio

We estimated the adjustment ratio by comparing surface observations with base case model simulations. **Figure 2a** describes the data processing procedures used to generate updated emissions for CMAQ simulation. We checked the validity of the observational data; only monitoring sites with more than 80% of observations available were included. To enable comparison, model data were also retrieved for the times and locations corresponding to observational data. Model data were discarded if paired observations were not available.

Both observations and model data were then assigned a grid cell identifier within the modeling domain and then averaged for each cell, a procedure designed to reduce the impact from unbalanced sampling in urban locations. Since most monitoring sites are located in high-population areas, the over-weighted urban observations could otherwise be applied to whole prefectures, including rural locations. **Figure 2b** shows an example cell-level concentration construction in the BTH region. Gray boxes indicate grid cells in the modeling domain, and all observational data within the same cell is averaged to one representative value, which is thereafter assigned to the location at the center of the cell.

Figure 3 describes the steps to generate the adjustment ratios to update current emission inputs for the model simulation. Data for June 2016 are shown. **Figure 3a** and **3b** show the spatial distribution of surface SO_2 concentrations from observations and the model. The differences between prefecture-level observations and the model are shown in **Figure 3c**. The current modeling domain includes 11 countries, 192 provinces (29 Chinese provinces and municipalities), and 3314 sub-divisions (309 Chinese prefectures). We decided to use the second-level administrative boundary, which is equivalent to the "prefecture" in China and the "county" in North America. Finally, **Figure 3d** shows the spatial distribution of the estimated adjustment ratios (observations divided by model), assuming a simple concentration-to-emissions ratio (often termed the beta value) of 1. That is, we assumed a percentage change in emissions would result in the same percentage change in concentration. The beta value will be further discussed later. In most areas, calculated ratios are less than 1, implying that the base model likely overestimates estimates, consistent with the declining trend in SO_2 emissions previous studies have often reported. Adjustment ratios over some inland locations are larger than 1, indicating increased SO_2 emissions.

3.3. Simulation with updated emissions

Adjusted SO_2 emissions are constructed by applying these adjustment ratios to the initial modeled SO_2 emissions. **Figure 4** compares SO_2 concentrations with initial and adjusted modeled emissions. Bias plots confirm the modeled SO_2 concentration improves when using adjusted emissions. For example, most strong overestimates over mega cities are removed after the emission-adjustment procedure. In general, all model-evaluation statistics are improved, as clearly shown in **Figure 4e** and **F**.

Several points remain which the current methodology cannot fully resolve. First, coastal areas could be improved by using a higher-resolution domain setting. Second, opposite bias signals in some areas can cancel each other, in which case the current method cannot resolve the locality of the emission source distribution. Third, large subdivisions with too small observational dataset can still be poorly modeled.

Time series of daily averaged SO_2 concentrations at monitoring sites over all of China and the four major locations of interest, along with SO_2 concentrations from the base and adjusted model runs, are shown in **Figure 5**. As expected, simulations clearly improve with the updated SO_2 emissions. Evaluative statistics show clear improvement throughout. Over all of China with 1332 monitoring sites, model bias improved from +4.07 ppb in the base run to -1.03 ppb in the adjusted run. Four megacities (BTH, YRD, PRD, and CHQ) where fractional biases seriously overestimated modeled SO_2 concentrations (by +196%, +246%, 196%, and +173%, respectively) also had dramatically improved model performance after adjustment (to misestimates by +8.5%, -10.8%, -13.7%, and -13.2%, respectively). These comparisons demonstrate that the suggested methodology improves model simulation by updating emissions. In general, the intensity and influence of SO_2 emissions are significant during the heating season (Meng et al., 2018), and the modeled results using the updated emissions confirm the seasonality of SO_2 emissions and concentration.

Figure 6 compares observed and simulated surface SO_2 concentrations for each Chinese prefecture. Out of 28 Chinese provinces and municipalities, modeled surface SO_2 concentrations are overestimated in 18 provinces, implying that the known emissions inventory might have overestimated SO_2 emissions in those provinces. Most provinces with high SO_2 emissions appear to be overestimated, implying that SO_2 emissions in those regions, which include highly industrialized areas, have been seriously reduced. This is consistent with recent reports of reduced SO_2 emissions from Chinese anthropogenic sources (van der A et al., 2017; Zhang et al., 2015).

3.4. Implications of Chinese emissions changes

Figure 7 shows the spatial distribution of recent changes in prefecture-level SO_2 concentrations for each season. The top panel shows the distribution of SO_2 concentration for each season, and the second to fourth rows present relative changes in prefecture-level SO_2 concentrations compared to 2015 levels. In 2015, SO_2 concentrations were highest in the first quarter (January–March) and lowest in the third quarter (July–September), showing typical seasonal variation.

In general, SO_2 concentrations are decreasing, especially in 2018. However, we have no evidence that this decrease is solely due to reduced emissions, nor has this decrease been clearly associated with any other factor, especially meteorological. A declining trend from 2015 is clear during the cold season compared to the warm season, suggesting a potential association with the residential emission sector (due to residential heating), but further studies are required to confirm this hypothesis.

We further estimated yearly variations of estimated SO_2 emissions over China during 2015-2018 using the approach developed in this study. **Figure 8** compares estimated SO_2 emissions from different emissions inventories and previous studies—Multi-resolution Emission Inventory for China (MEIC) v1.2, CREATE 2015, KORUS-AQ emissions versions 2.1 and 5, Koukouli et al. (2018) and Zheng et al. (2018)—with estimated SO_2 emissions from this study (Koukouli et al., 2018; Zheng et al., 2018). Interestingly, in 2015, the total amount of estimates SO_2 emission is very close to that of CREATE 2015. However, their spatial distribution is quite different. For example, our result estimates BTH SO_2 emissions as 1.8 Tg/year while CREATE 2015 has much higher emission amount, 3.5 Tg/year.

The estimate from this study is 19.3 Tg/year (18.1 Tg/year inside simulation domain) for 2016, based on the top-down approach estimated from surface concentration; note, however, that this study aimed to improve model performance and has not focused specifically on estimating accurate emission information. Therefore, this comparison should be taken as a guidance for relative emissions change, and should not be used for evaluation purpose. **Table 2** summarizes the estimated SO_2 emissions from each province**.**

As shown in **Figure 6**, one area with a notable discrepancy in SO_2 emissions is Shanxi province, located west of Beijing, which is well-known for having the largest coal reserves in China, along with nearly a hundred coal-powered power plants. The high SO_2 loadings southwest of BTH could be partially attributed to emissions from Shanxi. Song et al. (2014) reported that the successful operation of a flue gas desulfurization (FGD) system in Shanxi reduced SO_2 emissions from power plants from 2005 to 2010 but that its emissions had rebounded from 2011 to 2012 (Song and Yang, 2014). **Figure 7** also shows slightly increased SO_2 concentrations in Shanxi province recent years, compared to 2015 level.

Increased emissions alone could be due to emission control failures or to an explicit policy to move emission sources from the core BTH region to adjacent regions. Fang et al. (2019) reported that the Chinese government's emission-abatement policy has led to temporary increases in emissions in neighboring provinces to the regions of main interest (Fang et al., 2019). After investigating the development of other emission sources in Shanxi, Song et al. (2014) concluded that the rapid expansion of high coal-consumption industries are responsible for the rise in 2011–2012 SO_2 emissions (Song and Yang, 2014). If emissions sources in the BTH region have been moved to Shanxi, this is notable in terms of international source-receptor relationship. In South Korea, there has been rumors in the social network services that the Chinese government has pushed pollution-emitting facilities to the Shandong area, which is close to South Korea. As addressed in Kim et al. (2018) (Kim et al., 2018), there is no evidence of increased SO_2 or NO_x emissions from Shandong province, and actual observations may suggest that BTH emissions have moved to the west (i.e. Shanxi) not to the east of BTH (i.e. Shandong). Zhang et al. (2015) also reported considerable differences in SO_2 emission-control efficiency by region in China (Zhang et al., 2015).

4. **Conclusion**

We have developed a data-processing framework to update SO_2 emissions using observations from surface monitoring sites. Thanks to enhanced coverage surface observation networks, we were able to process prefecture-level observational data. Updated SO_2 emissions were generated by applying adjustment ratios to prefecture-level SO_2 concentrations between observations and the model. We chose a prefecture-level adjustment to include the effects of local transport.

Using the suggested method, we conducted CMAQ simulations with updated SO_2 emissions. With this adjustment method, CMAQ very well reproduces both spatial and seasonal variations. Using this method, we further estimated the amount of SO_2 emissions. For most major emission sources, including megacities like BTH, YRD, PRD, and Chongqing city, our results suggest serious reductions in SO_2 emissions, consistent with a stringent SO_2 emission-control policy by the Chinese government. On the other hand, in some areas we have estimated increased SO_2 emissions, most notably in Shanxi province.

We conclude that frequent updates to anthropogenic emissions sources are required to improve the performance of regional air-quality modeling systems and forecasts. Top-down estimation of anthropogenic emissions using actual observational data can greatly improve simulation accuracy.

5. **References**

Binkowski, F.S., 2003. Models-3 Community Multiscale Air Quality (CMAQ) model aerosol component 1. Model description. J. Geophys. Res. 108, 4183. https://doi.org/10.1029/2001JD001409

Byun, D., Schere, K.L., 2006. Review of the Governing Equations, Computational Algorithms, and Other Components of the Models-3 Community Multiscale Air Quality (CMAQ) Modeling System. Appl. Mech. Rev. 59, 51. https://doi.org/10.1115/1.2128636

Carter, W.P.L., 2003. The SAPRC-99 Chemical Mechanism and Updated VOC Reactivity Scales [WWW Document]. URL http://www.cert.ucr.edu/~carter/reactdat.htm

Chang, J.S., Brost, R.A., Isaksen, I.S.A., Madronich, S., Middleton, P., Stockwell, W.R., Walcek, C.J., 1987. A three-dimensional Eulerian acid deposition model: Physical concepts and formulation. J. Geophys. Res. 92, 14681. https://doi.org/10.1029/JD092iD12p14681

Chen, F., Dudhia, J., 2001. Coupling an Advanced Land Surface–Hydrology Model with the Penn State–NCAR MM5 Modeling System. Part I: Model Implementation and Sensitivity. Mon. Weather Rev. 129, 569–585. https://doi.org/10.1175/1520-0493(2001)129<0569:CAALSH>2.0.CO;2

Chen, R., Huang, W., Wong, C.-M., Wang, Z., Quoc Thach, T., Chen, B., Kan, H., 2012. Short-term exposure to sulfur dioxide and daily mortality in 17 Chinese cities: The China air pollution and health effects study (CAPES). Environ. Res. 118, 101–106. https://doi.org/10.1016/j.envres.2012.07.003

EPA, 2008. Integrated Science Assessment (ISA) for Oxides of Nitrogen and Sulfur - Environmental Criteria (Second External Review Draft, Aug 2008).

Fang, D., Chen, B., Hubacek, K., Ni, R., Chen, L., Feng, K., Lin, J., 2019. Clean air for some: Unintended spillover effects of regional air pollution policies. Sci. Adv. 5, eaav4707. https://doi.org/10.1126/sciadv.aav4707

Fioletov, V., McLinden, C.A., Kharol, S.K., Krotkov, N.A., Li, C., Joiner, J., Moran, M.D., Vet, R., Visschedijk, A.J.H., Denier van der Gon, H.A.C., 2017. Multi-source SO 2 emission retrievals and consistency of satellite and surface measurements with reported emissions. Atmos. Chem. Phys. 17, 12597–12616. https://doi.org/10.5194/acp-17-12597-2017

Fioletov, V.E., McLinden, C. a., Krotkov, N., Yang, K., Loyola, D.G., Valks, P., Theys, N., Van Roozendael, M., Nowlan, C.R., Chance, K., Liu, X., Lee, C., Martin, R. V., 2013. Application of OMI, SCIAMACHY, and GOME-2 satellite SO 2 retrievals for detection of large emission sources. J. Geophys. Res. Atmos. 118, 11,399-11,418. https://doi.org/10.1002/jgrd.50826

Fioletov, V.E., McLinden, C.A., Krotkov, N., Li, C., Joiner, J., Theys, N., Carn, S., Moran, M.D., 2016. A global catalogue of large SO 2 sources and emissions derived from the Ozone Monitoring Instrument. Atmos. Chem. Phys. 16, 11497–11519. https://doi.org/10.5194/acp-16-11497-2016

Flower, V.J.B., Oommen, T., Carn, S.A., 2016. Improving global detection of volcanic eruptions using the Ozone Monitoring Instrument (OMI). Atmos. Meas. Tech. 9, 1–24. https://doi.org/10.5194/amt-9-5487-2016

Georgoulias, A.K., Balis, D., Koukouli, M.E., Meleti, C., Bais, A., Zerefos, C., 2009. A study of the total atmospheric sulfur dioxide load using ground-based measurements and the satellite derived Sulfur Dioxide Index. Atmos. Environ. 43, 1693–1701. https://doi.org/10.1016/j.atmosenv.2008.12.012

Harris, E., Sinha, B., van Pinxteren, D., Tilgner, A., Fomba, K.W., Schneider, J., Roth, A., Gnauk, T., Fahlbusch, B., Mertes, S., Lee, T., Collett, J., Foley, S., Borrmann, S., Hoppe, P., Herrmann, H., 2013. Enhanced Role of Transition Metal Ion Catalysis During In-Cloud Oxidation of SO2. Science (80-.). 340, 727–730. https://doi.org/10.1126/science.1230911

Hertel, O., Berkowicz, R., Christensen, J., Hov, Ø., 1993. Test of two numerical schemes for use in atmospheric transport-chemistry models. Atmos. Environ. Part A. Gen. Top. 27, 2591–2611. https://doi.org/10.1016/0960-1686(93)90032-T

Hong, S.-Y., Dudhia, J., Chen, S.-H., 2004. A Revised Approach to Ice Microphysical Processes for the Bulk Parameterization of Clouds and Precipitation. Mon. Weather Rev. 132, 103–120. https://doi.org/10.1175/1520-0493(2004)132<0103:ARATIM>2.0.CO;2

Hong, S.-Y., Noh, Y., Dudhia, J., 2006. A new vertical diffusion package with an explicit treatment of entrainment processes. Mon. Weather Rev. 134, 2318–2341. https://doi.org/10.1175/MWR3199.1

Huanhuan, Y., Liangfu, C., Lin, S., Jinhua, T., Chao, Y., 2014. SO 2 columns over China: Temporal and spatial variations using OMI and GOME-2 observations. IOP Conf. Ser. Earth Environ. Sci. 17, 012027. https://doi.org/10.1088/1755-1315/17/1/012027

Jang, Y., Lee, Y., Kim, J., Kim, Y., Woo, J.-H.H., 2019. Improvement China Point Source for Improving Bottom-Up Emission Inventory. Asia-Pacific J. Atmos. Sci. https://doi.org/10.1007/s13143-019-00115-y

Kain, J.S., 2004. The Kain–Fritsch Convective Parameterization: An Update. J. Appl. Meteorol. 43, 170–181. https://doi.org/10.1175/1520-0450(2004)043<0170:TKCPAU>2.0.CO;2

Kang, H., Zhu, B., van der A, R.J., Zhu, C., de Leeuw, G., Hou, X., Gao, J., 2019. Natural and anthropogenic contributions to long-term variations of SO2, NO2, CO, and AOD over East China. Atmos. Res. 215, 284–293. https://doi.org/10.1016/j.atmosres.2018.09.012

Kim, H., Lee, S.-M., Chai, T., Ngan, F., Pan, L., Lee, P., 2018. A Conservative Downscaling of Satellite-Detected Chemical Compositions: NO2 Column Densities of OMI, GOME-2, and CMAQ. Remote Sens. 10, 1001. https://doi.org/10.3390/rs10071001

Kim, H.C., Kim, S., Kim, B.-U., Jin, C.-S., Hong, S., Park, R., Son, S.-W., Bae, C., Bae, M., Song, C.-K., Stein, A., 2017. Recent increase of surface particulate matter concentrations in the Seoul Metropolitan Area, Korea. Sci. Rep. 7, 4710. https://doi.org/10.1038/s41598-017-05092-8

Kim, H.C., Kwon, S., Kim, B.-U., Kim, S., 2018. Review of Shandong Peninsular Emissions Change and South Korean Air Quality. J. Korean Soc. Atmos. Environ. 34, 356–365. https://doi.org/10.5572/KOSAE.2018.34.2.356

Kim, H.C., Lee, P., Judd, L., Pan, L., Lefer, B., 2016. OMI NO 2 column densities over North American urban cities: the effect of satellite footprint resolution. Geosci. Model Dev. 9, 1111–1123. https://doi.org/10.5194/gmd-9-1111-2016

Klimont, Z., Smith, S.J., Cofala, J., 2013. The last decade of global anthropogenic sulfur dioxide: 2000–2011 emissions. Environ. Res. Lett. 8, 014003. https://doi.org/10.1088/1748-9326/8/1/014003

Koukouli, M.E., Balis, D.S., van der A, R.J., Theys, N., Hedelt, P., Richter, A., Krotkov, N., Li, C., Taylor, M., 2016. Anthropogenic sulphur dioxide load over China as observed from different satellite sensors. Atmos. Environ. 145, 45–59. https://doi.org/10.1016/j.atmosenv.2016.09.007

Koukouli, M.E., Theys, N., Ding, J., Zyrichidou, I., Mijling, B., Balis, D., van der A, R.J., 2018. Updated SO 2 emission estimates over China using OMI/Aura observations. Atmos. Meas. Tech. 11, 1817–1832. https://doi.org/10.5194/amt-11-1817-2018

Krotkov, N. a., McLinden, C. a., Li, C., Lamsal, L.N., Celarier, E. a., Marchenko, S. V., Swartz, W.H., Bucsela, E.J., Joiner, J., Duncan, B.N., Boersma, K.F., Veefkind, J.P., Levelt, P.F., Fioletov, V.E., Dickerson, R.R., He, H., Lu, Z., Streets, D.G., 2016. Aura OMI observations of regional SO_2 and NO_2 pollution changes from 2005 to 2015. Atmos. Chem. Phys. 16, 4605–4629. https://doi.org/10.5194/acp-16-4605-2016

Krotkov, N.A., McLinden, C.A., Li, C., Lamsal, L.N., Celarier, E.A., Marchenko, S. V., Swartz, W.H., Bucsela, E.J., Joiner, J., Duncan, B.N., Boersma, K.F., Veefkind, J.P., Levelt, P.F., Fioletov, V.E., Dickerson, R.R., He, H., Lu, Z., Streets, D.G., 2016. Aura OMI observations of regional SO2 and NO2 pollution changes from 2005 to 2015. Atmos. Chem. Phys. 16, 4605–4629. https://doi.org/10.5194/acp-16-4605-2016

Krueger, A., Krotkov, N., Carn, S., 2008. El Chichon: The genesis of volcanic sulfur dioxide monitoring from space. J. Volcanol. Geotherm. Res. 175, 408–414. https://doi.org/10.1016/j.jvolgeores.2008.02.026

Lee, C., Martin, R. V., van Donkelaar, A., Lee, H., Dickerson, R.R., Hains, J.C., Krotkov, N., Richter, A., Vinnikov, K., Schwab, J.J., 2011. SO 2 emissions and lifetimes: Estimates from inverse modeling using in situ and global, space-based (SCIAMACHY and OMI) observations. J. Geophys. Res. 116, 14758. https://doi.org/10.1029/2010JD014758

Li, M., Liu, H., Geng, G., Hong, C., Liu, F., Song, Y., Tong, D., Zheng, B., Cui, H., Man, H., Zhang, Q., He, K., 2017a. Anthropogenic emission inventories in China: A review. Natl. Sci. Rev. 4, 834–866. https://doi.org/10.1093/nsr/nwx150

Li, M., Zhang, Q., Kurokawa, J., Woo, J.-H., He, K., Lu, Z., Ohara, T., Song, Y., Streets, D.G., Carmichael, G.R., Cheng, Y., Hong, C., Huo, H., Jiang, X., Kang, S., Liu, F., Su, H., Zheng, B., 2017b. MIX: a mosaic Asian anthropogenic emission inventory under the international collaboration framework of the MICS-Asia and HTAP. Atmos. Chem. Phys. 17, 935–963. https://doi.org/10.5194/acp-17-935-2017

Lin, M., Tao, J., Chan, C.-Y., Cao, J.-J., Zhang, Z.-S., Zhu, L.-H., Zhang, R.-J., 2012. Regression Analyses between Recent Air Quality and Visibility Changes in Megacities at Four Haze Regions in China. Aerosol Air Qual. Res. 12, 1049–1061. https://doi.org/10.4209/aaqr.2011.11.0220

Lin, Y.-H., Knipping, E.M., Edgerton, E.S., Shaw, S.L., Surratt, J.D., 2013. Investigating the influences of SO_2 and NH_3 levels on isoprene-derived secondary organic aerosol formation using conditional sampling approaches. Atmos. Chem. Phys. 13, 8457–8470. https://doi.org/10.5194/acp-13-8457-2013

Liu, F., Choi, S., Li, C., Fioletov, V.E., McLinden, C.A., Joiner, J., Krotkov, N.A., Bian, H., Janssens-Maenhout, G., Darmenov, A.S., da Silva, A.M., 2018. A new global anthropogenic SO_2 emission inventory for the last decade: a mosaic of satellite-derived and bottom-up emissions. Atmos. Chem. Phys. 18, 16571–16586. https://doi.org/10.5194/acp-18-16571-2018

Liu, L., Zhang, B., Bi, J., 2012. Reforming China's multi-level environmental governance: Lessons from the 11th Five-Year Plan. Environ. Sci. Policy 21, 106–111. https://doi.org/10.1016/j.envsci.2012.05.001

Liu, X., Lin, B., Zhang, Y., 2016. Sulfur dioxide emission reduction of power plants in China: current policies and implications. J. Clean. Prod. 113, 133–143. https://doi.org/10.1016/j.jclepro.2015.12.046

Louis, J.-F., 1979. A parametric model of vertical eddy fluxes in the atmosphere. Boundary-Layer Meteorol. 17, 187–202. https://doi.org/10.1007/BF00117978

Meng, K., Xu, Xiangde, Cheng, X., Xu, Xiaobin, Qu, X., Zhu, W., Ma, C., Yang, Y., Zhao, Y., 2018. Spatio-temporal variations in SO_2 and NO_2 emissions caused by heating over the Beijing-Tianjin-Hebei Region constrained by an adaptive nudging method with OMI data. Sci. Total Environ. 642, 543–552. https://doi.org/10.1016/j.scitotenv.2018.06.021

Miao, Y., Guo, J., Liu, S., Liu, H., Zhang, G., Yan, Y., He, J., 2017. Relay transport of aerosols to Beijing-Tianjin-Hebei region by multi-scale atmospheric circulations. Atmos. Environ. 165, 35–45. https://doi.org/10.1016/j.atmosenv.2017.06.032

NCEP, 2000. NCEP FNL Operational Model Global Tropospheric Analyses, continuing from July 1999. Research Data Archive at the National Center for Atmospheric Research, Computational and Information Systems Laboratory. https://doi.org/10.5065/D6M043C6

Otte, T.L., Pleim, J.E., 2010. The Meteorology-Chemistry Interface Processor (MCIP) for the CMAQ modeling system: updates through MCIPv3.4.1. Geosci. Model Dev. 3, 243–256. https://doi.org/10.5194/gmd-3-243-2010

Park, J., Cho, S.Y., 1998. A long range transport of SO_2 and Sulfate between Korea and East China. Atmos. Environ. 32, 2745–2756. https://doi.org/10.1016/S1352-2310(98)00034-X

Qu, Y., An, J., He, Y., Zheng, J., 2016. An overview of emissions of SO_2 and NO_x and the long-range transport of oxidized sulfur and nitrogen pollutants in East Asia. J. Environ. Sci. 44, 13–25. https://doi.org/10.1016/j.jes.2015.08.028

Qu, Z., Henze, D.K., Li, C., Theys, N., Wang, Y., Wang, J., Wang, W., Han, J., Shim, C., Dickerson, R.R., Ren, X., 2019. SO_2 Emission Estimates Using OMI SO_2 Retrievals for 2005–2017. J. Geophys. Res. Atmos. 124, 8336–8359. https://doi.org/10.1029/2019JD030243

Schreifels, J.J., Fu, Y., Wilson, E.J., 2012. Sulfur dioxide control in China: policy evolution during the 10th and 11th Five-year Plans and lessons for the future. Energy Policy 48, 779–789. https://doi.org/10.1016/j.enpol.2012.06.015

Silver, B., Reddington, C.L., Arnold, S.R., Spracklen, D. V, 2018. Substantial changes in air pollution across China during 2015–2017. Environ. Res. Lett. 13, 114012. https://doi.org/10.1088/1748-9326/aae718

Skamarock, W.C., Klemp, J.B., 2008. A time-split nonhydrostatic atmospheric model for weather research and forecasting applications. J. Comput. Phys. 227, 3465–3485. https://doi.org/10.1016/j.jcp.2007.01.037

Song, H., Yang, M., 2014. Analysis on Effectiveness of SO2 Emission Reduction in Shanxi, China by Satellite Remote Sensing. Atmosphere (Basel). 5, 830–846. https://doi.org/10.3390/atmos5040830

Spinei, E., Carn, S.A., Krotkov, N. a., Mount, G.H., Yang, K., Krueger, A., 2010. Validation of ozone monitoring instrument SO 2 measurements in the Okmok volcanic cloud over Pullman, WA, July 2008. J. Geophys. Res. 115, D00L08. https://doi.org/10.1029/2009JD013492

Stern, D.I., 2005. Global sulfur emissions from 1850 to 2000. Chemosphere 58, 163–175. https://doi.org/10.1016/j.chemosphere.2004.08.022

Theys, N., Hedelt, P., De Smedt, I., Lerot, C., Yu, H., Vlietinck, J., Pedergnana, M., Arellano, S., Galle, B., Fernandez, D., Carlito, C.J.M., Barrington, C., Taisne, B., Delgado-Granados, H., Loyola, D., Van Roozendael, M., 2019. Global monitoring of volcanic SO2 degassing with unprecedented resolution from TROPOMI onboard Sentinel-5 Precursor. Sci. Rep. 9, 2643. https://doi.org/10.1038/s41598-019-39279-y

van der A, R.J., Mijling, B., Ding, J., Koukouli, M.E., Liu, F., Li, Q., Mao, H., Theys, N., 2017. Cleaning up the air: effectiveness of air quality policy for SO 2 and NO x emissions in China. Atmos. Chem. Phys. 17, 1775–1789. https://doi.org/10.5194/acp-17-1775-2017

Wang, Y.Y., Wang, J., Xu, X., Henze, D.K., Wang, Y.Y., Qu, Z., 2016. A new approach for monthly updates of anthropogenic sulfur dioxide emissions from space: Application to China and implications for air quality forecasts. Geophys. Res. Lett. 43, 9931–9938. https://doi.org/10.1002/2016GL070204

Wang, Z., Zheng, F., Zhang, W., Wang, S., 2018. Analysis of SO 2 Pollution Changes of Beijing-Tianjin-Hebei Region over China Based on OMI Observations from 2006 to 2017. Adv. Meteorol. 2018, 1–15. https://doi.org/10.1155/2018/8746068

Xiao, Y., Song, Y., Wu, X., 2018. How Far Has China's Urbanization Gone? Sustainability 10, 2953. https://doi.org/10.3390/su10082953

Yamartino, R.J., 1993. Nonnegative, Conserved Scalar Transport Using Grid-Cell-centered, Spectrally Constrained Blackman Cubics for Applications on a Variable-Thickness Mesh. Mon. Weather Rev. 121, 753–763. https://doi.org/10.1175/1520-0493(1993)121<0753:NCSTUG>2.0.CO;2

Ying, Q., Wu, L., Zhang, H., 2014. Local and inter-regional contributions to PM2.5 nitrate and sulfate in China. Atmos. Environ. 94, 582–592. https://doi.org/10.1016/j.atmosenv.2014.05.078

Zhang, Q.Q., Wang, Y., Ma, Q., Yao, Y., Xie, Y., He, K., 2015. Regional differences in Chinese SO 2 emission control efficiency and policy implications. Atmos. Chem. Phys. 15, 6521–6533. https://doi.org/10.5194/acp-15-6521-2015

Zhang, Y., Li, C., Krotkov, N.A., Joiner, J., Fioletov, V., McLinden, C., 2017. Continuation of long-term global SO₂ pollution monitoring from OMI to OMPS. Atmos. Meas. Tech. 10, 1495–1509. https://doi.org/10.5194/amt-10-1495-2017

Zheng, B., Tong, D., Li, M., Liu, F., Hong, C., Geng, G., Li, H., Li, X., Peng, L., Qi, J., Yan, L., Zhang, Y., Zhao, H., Zheng, Y., He, K., Zhang, Q., 2018. Trends in China's anthropogenic emissions since 2010 as the consequence of clean air actions. Atmos. Chem. Phys. 18, 14095–14111. https://doi.org/10.5194/acp-18-14095-2018

Table 1. Physical options for meteorological and chemical simulations.

Model	Physical options	Descriptions
WRF v3.4.1	Initial field	FNL (NCEP, 2000)
	Microphysics	WSM6 (Hong et al., 2004)
	Cumulus scheme	Kain-Fritsch (Kain, 2004)
	Land surface model scheme	NOAH (Chen and Dudhia, 2001)
	Planetary boundary layer scheme	YSU (Hong et al., 2006)
CMAQ v4.7.1	Chemical mechanism	SAPRC99 (Carter, 2003)
	Chemical solver	EBI (Hertel et al., 1993)
	Aerosol module	AERO5 (Binkowski, 2003)
	Advection scheme	YAMO (Yamartino, 1993)
	Horizontal diffusion	Multiscale (Louis, 1979)
	Vertical diffusion	Eddy (Louis, 1979)
	Cloud scheme	RADM (Chang et al., 1987)

Table 2. Base (CREATE 2015) and estimated, province-level Chinese SO_2 emissions (Unit: KTon/year).

Region	Base	Adjusted	Region	Base	Adjusted
Heilongjia	486	591	Fujian	453	302
Jilin	495	437	Jiangxi	598	732
Liaoning	1,600	1,267	Henan	1,634	1,195
NeiMongol	1,256	1,151	Hubei	1,098	493
Hebei	2,549	1,189	Hunan	811	730
Beijing	478	46	Guangdong	1,273	630
Tianjin	587	107	Guangxi	713	983
Shanxi	1,549	1,835	Shaanxi	916	608
Shandong	2,337	1,694	NingxiaHui	230	444
Jiangsu	1,472	681	Chongqing	926	192
Shanghai	1,463	163	Sichuan	866	531
Zhejiang	1,242	418	Guizhou	540	856
Anhui	823	519	Yunnan	210	388

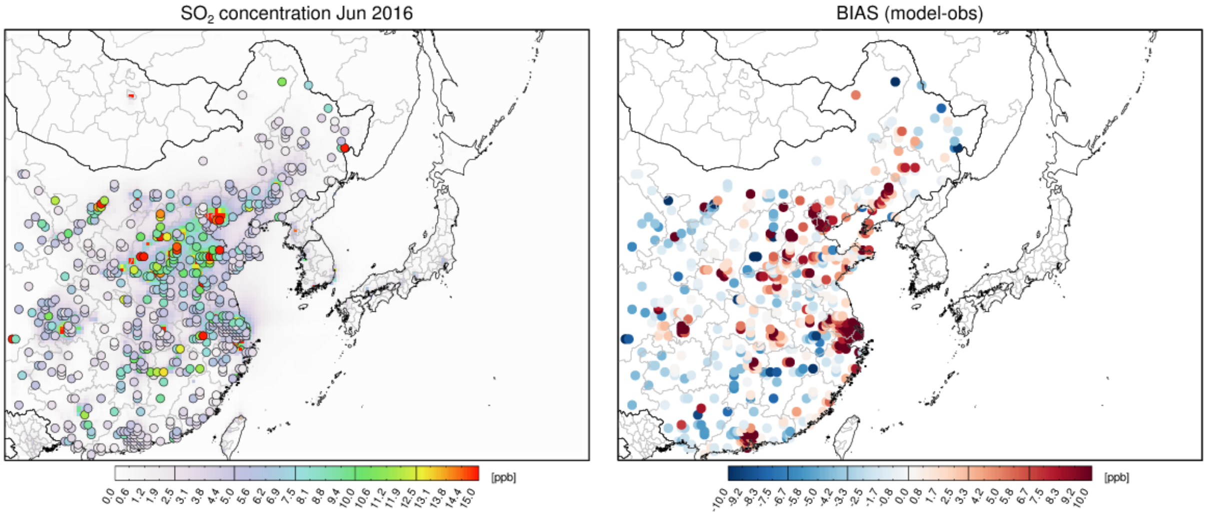

Figure 1. Spatial distribution of modeled SO_2 concentrations overlaid by surface monitoring sites over China in June 2016 (left) and their biases (right).

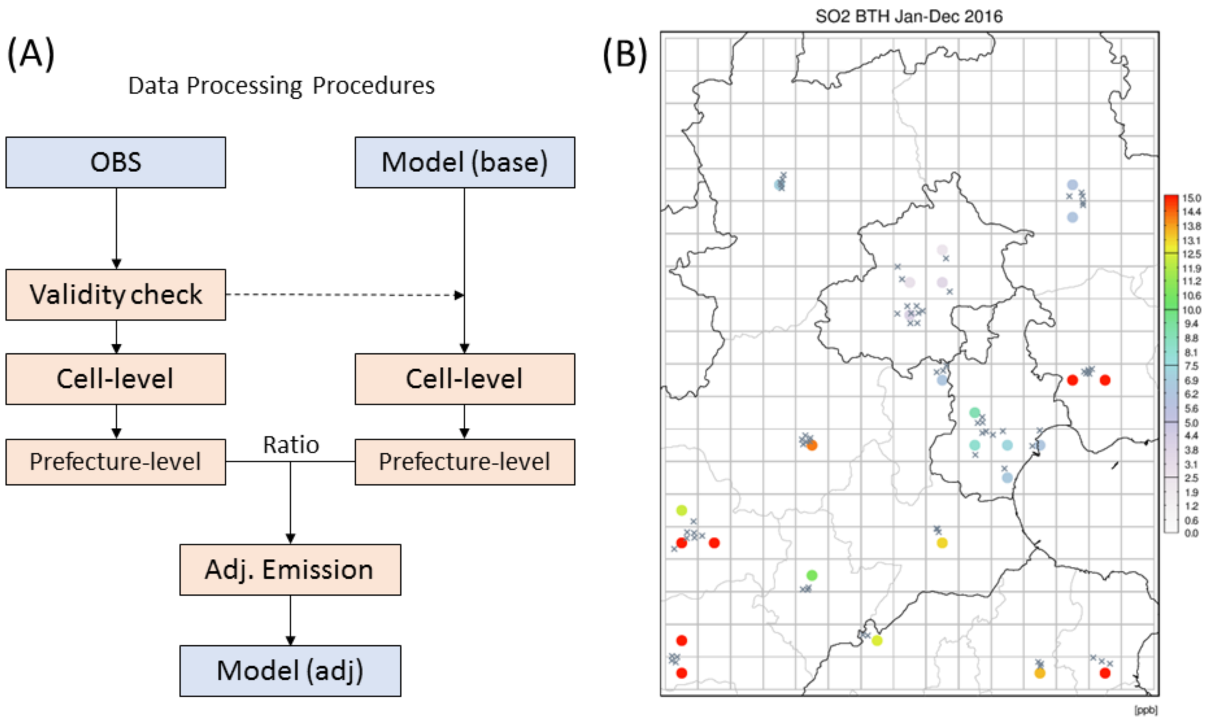

Figure 2. Schematic diagram of data processing for emission adjustment (left), and a zoomed-in map of surface-monitoring site locations and "cell-level" averaged SO_2 concentrations in the BTH region (right).

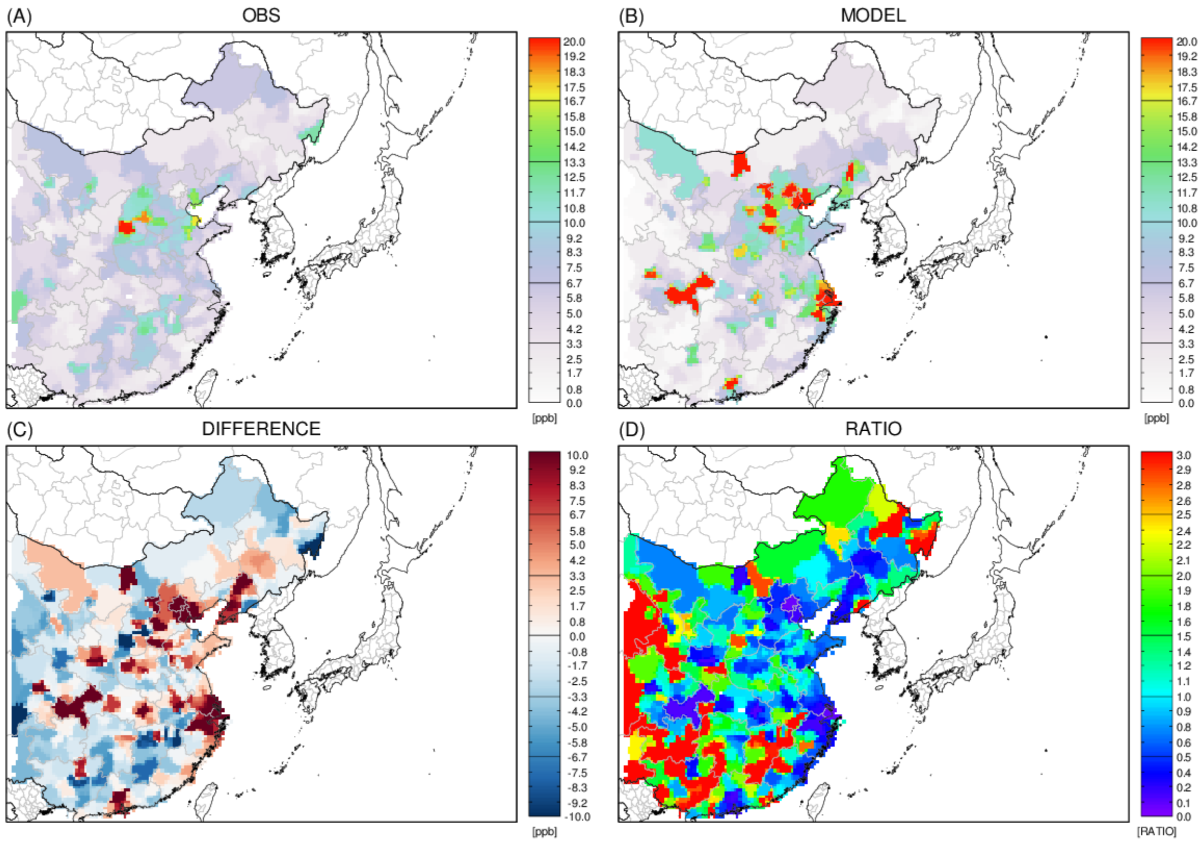

Figure 3. Calculation of emissions adjustment ratio. Shown are surface SO_2 concentrations for June 2016 from (a) observation, (b) model simulation, (c) their difference, and (d) the adjustment ratios (observations/model).

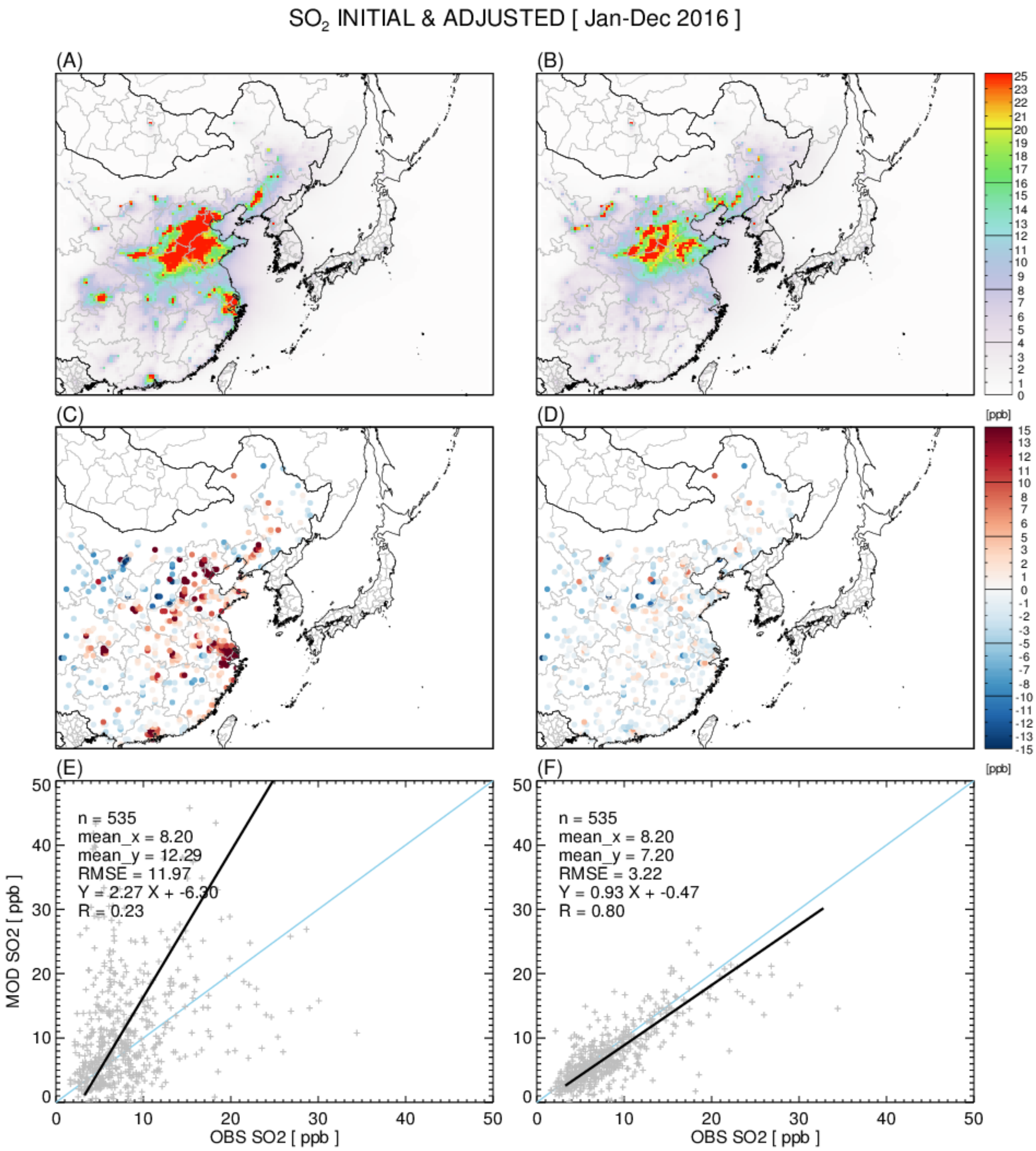

Figure 4. Performance evaluation of models run with initial emissions inventory (left) and adjusted emissions (right). Also shown are spatial distributions of simulated SO2 concentrations (top) and biases (middle), as well as scatter plot comparisons for initial (bottom-left) and adjusted (bottom-right) emissions for January to December 2016.

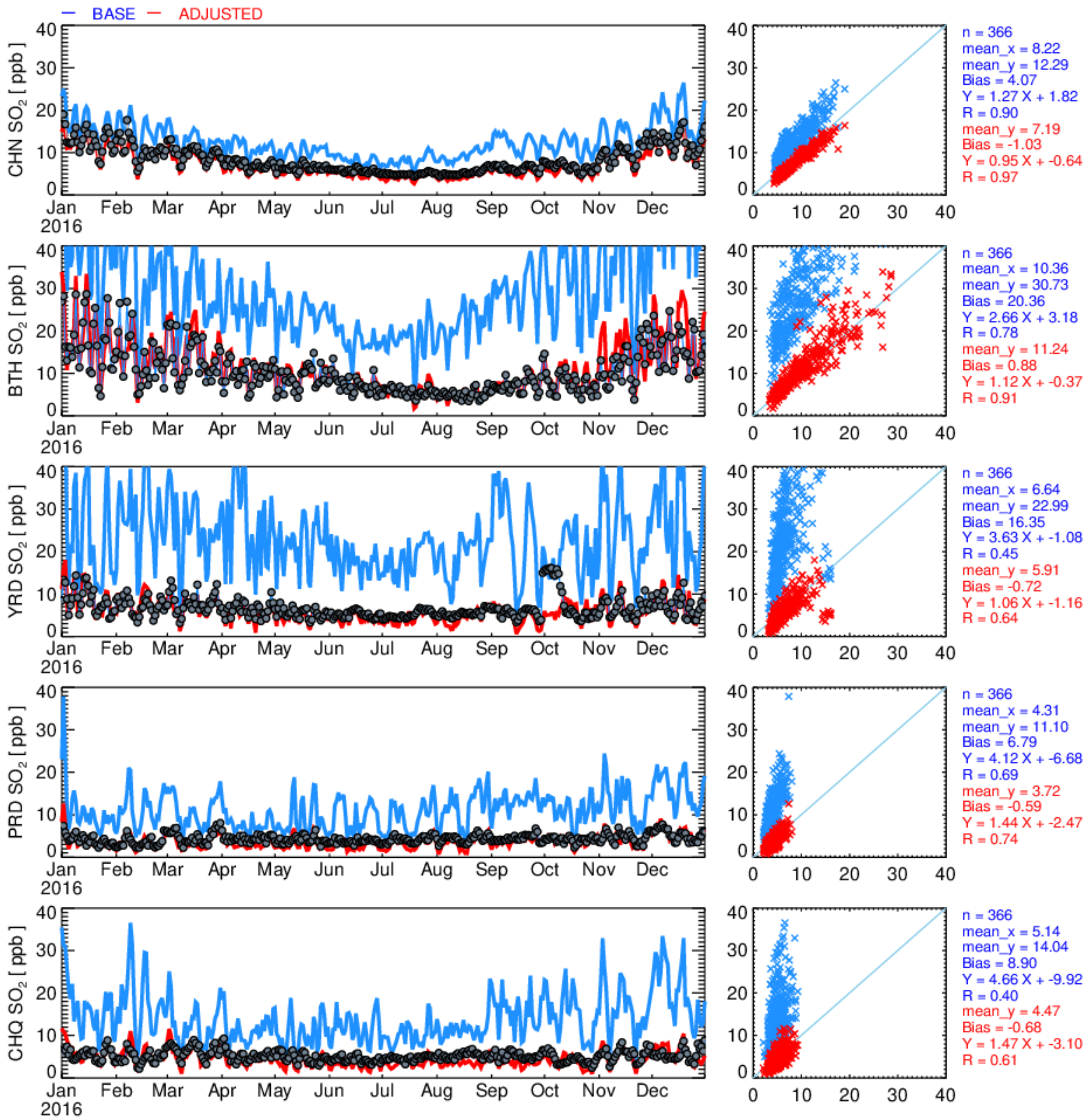

Figure 5. Time series of daily mean SO_2 concentrations over China (CHN), BTH, YRD, PRD, and Chongqing (CHQ) areas with base and adjusted model runs.

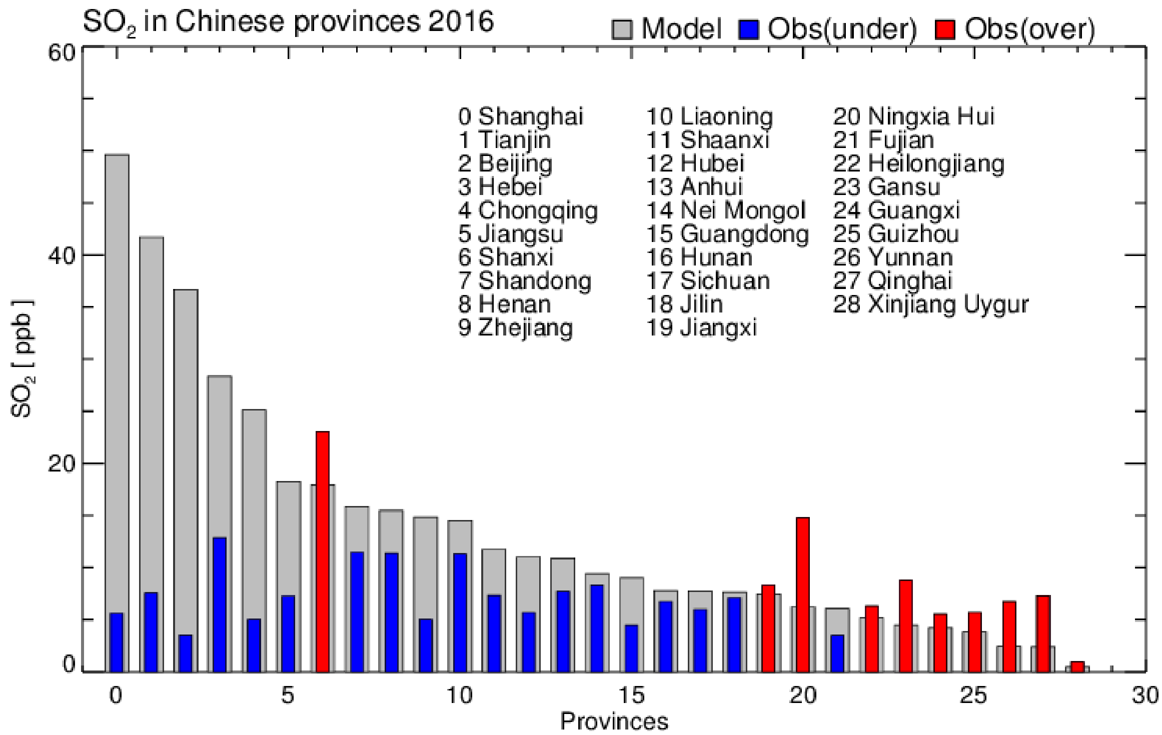

Figure 6. Comparison of modeled and observed SO_2 concentrations in 29 Chinese provinces during 2016. CREATE emissions before adjustment were used in the model.

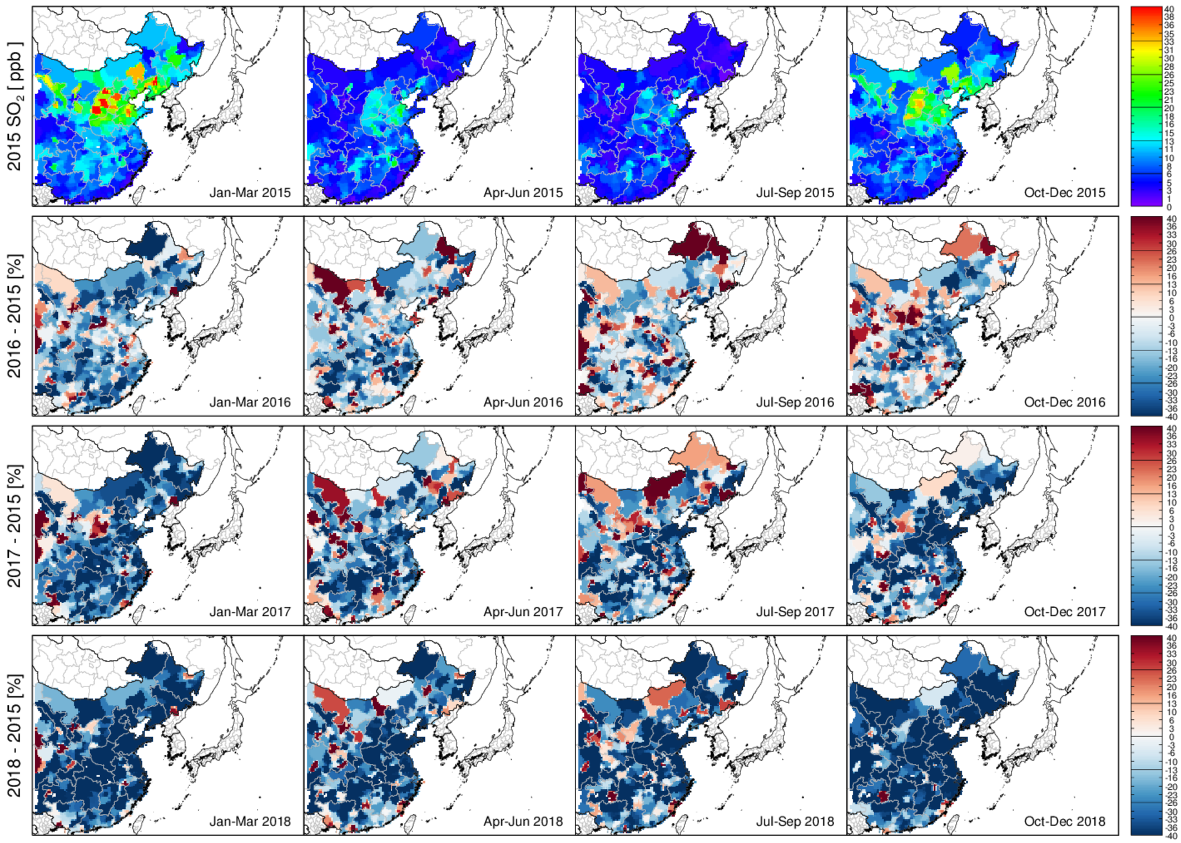

Figure 7. Spatial distributions of 2015 surface SO_2 concentrations averaged over each season (January–March, April–June, July–September, and October–December) (top row), and percentage changes from 2015 to 2016, 2017 and 2018 (2nd-4th row).

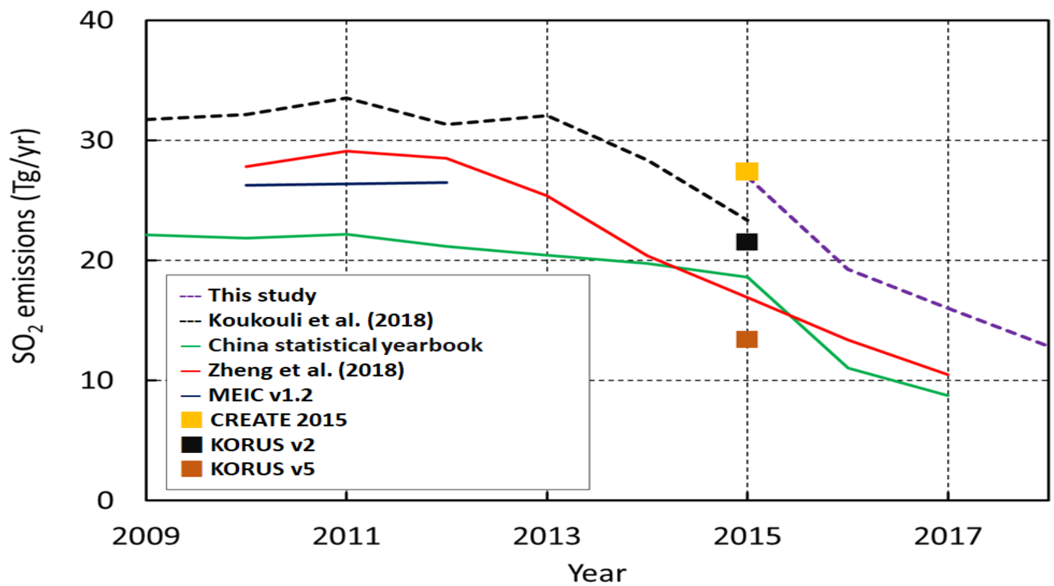

Figure 8. Comparison of estimates of Chinese SO_2 emissions based on emissions inventories and as estimated in this study.